MINERALOGICAL MAGAZINE, JUNE 1986, VOL. 50, PP. 271-7

Chemistry, optics, and crystal growth of milarite from Strzegom, Poland

J. JANECZEK

Department of Earth Sciences, Silesian University, Mielczarskiego 60, 41-200 Sosnowiec, Poland

ABSTRACT. Milarite was found in a cavity of a small pegmatitic segregation in association with albite, stilpnomelane and chabazite. Hexagonal, well-shaped crystals of milarite up to 4 mm in length are transparent, pale green in colour, and show bright green cathodoluminescence. The refractive indices are: $\omega = 1.535$, $\varepsilon = 1.534$(Na). D = 2.55 g cm^{-3}. The unit cell dimensions are: a 10.418(4), c 13.817(7) Å, V 1298.7 Å^3. Anomalous biaxial sectors and birefringent optical patterns are visible in basal section. 2V varies from 34° in the {0001} sector to 64° in {10$\bar{1}$1} sector. OAP azimuths are related to the external hexagonal symmetry of the crystals. Microprobe analyses of sections perpendicular and parallel to the c-axis revealed a uniform distribution of alkalis, mainly K_2O, whereas CaO and Al_2O_3 contents are slightly higher in prismatic and pyramidal sectors than in the basal sector, but no systematic chemical zoning can be distinguished. The Al_2O_3 content decreases in the outer zone of the crystal studied due to Be–Al substitution. The average 'anhydrous' chemical formula of the Strzegom milarite is: $(K_{0.98}Na_{0.01})Ca_{1.93}Mn_{0.02}(Be_{2.16}Al_{0.93})(Si_{12}O_{30})$. Infra-red data indicate the presence of H_2O molecules in the milarite. Internal growth structures of the crystals indicate rhythmic fluctuations of the growth rate resulting in an internal strain, inducing anomalous optical patterns. HRTEM study did not reveal any significant distortion of the milarite lattice.

KEYWORDS: milarite, crystal growth, Strzegom, Poland.

MILARITE, $(K,Na)Ca_2(Be_2Al)Si_{12}O_{30}0.75H_2O$ is a relatively rare mineral interesting for its anomalous optical properties and compositional variability within single crystals. Although the crystal structure and relationship between chemical composition and physical properties of milarite have been established (Bakanin *et al.*, 1974; Černy *et al.*, 1980), the existing data are still insufficient to explain the anomalous optical behaviour of this mineral.

A new occurrence of milarite from Poland was found in a granite quarry nearby Strzegom, SW Poland. Preliminary data on this mineral were briefly reported elsewhere (Janeczek 1984). The aim of this paper is to describe the milarite from Poland in detail, focusing attention on the chemical and optical heterogeneity within a single crystal.

Occurrence. A few crystals of milarite, associated with cleavelandite, stilpnomelane, and chabazite were found in a cavity in a small (30 × 20 × 15 cm) pegmatitic segregation that occurred in the form of a lenticular body narrowing to a vug lined with a fibrous bavenite, epidote, and stilbite. The mineral assemblage indicates that differentiation of the fluid composition took place within the pegmatite. The concentration of Ca ions was apparently higher in the vug, inducing rapid nucleation and growth of bavenite and epidote, whereas milarite has been formed from a more alkaline solution but in the presence of Ca ions. Both bavenite and milarite are undoubtedly primary minerals in the Strzegom pegmatites.

The sequence of hydrothermal crystallization in the cavity has been deduced to be as follows: cleavelandite (epitaxially overgrown on microcline), stilpnomelane, milarite, chabazite. Aggregates of stilpnomelane, now included in the cores of the crystals, were probably the crystallization centres.

Physical and optical properties. Milarite occurs as well-shaped, hexagonal crystals, sometimes doubly terminated, up to 4 mm in length and 2 mm in width, although typically they are about 2 mm long and 0.5 to 1 mm in thickness. The crystals are transparent, pale green and show bright green cathodoluminescence. They have a simple morphology with well developed (11$\bar{2}$0), (0001), and (10$\bar{1}$1) faces. The unit cell parameters obtained from the X-ray powder pattern of one crystal are: a 10.418(4), c 13.817(7) Å, V 1298.7 Å^3, c/a 1.326. The average density of two crystals determined by flotation in heavy liquids is 2.553 g cm^{-3}.

Almost every kind of optical anomaly reported for milarite can be easily observed in the Strzegom samples. The crystals show biaxial sectors in sections perpendicular to the c-axis (figs. 1 and 2). Zonal sectors corresponding to the prism faces form a rim surrounding pyramidal and basal sectors.

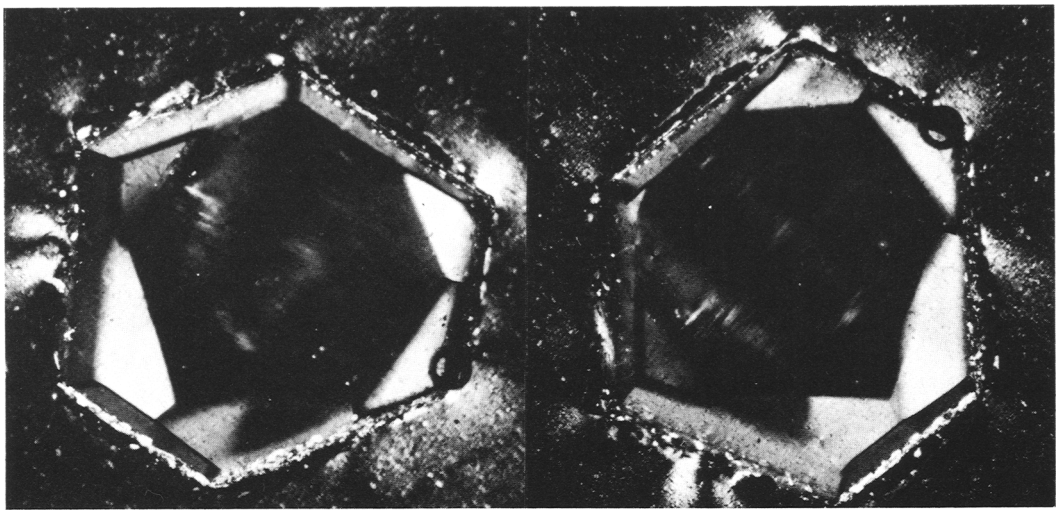

FIG. 1. Crystal of milarite (M4) showing a Moiré-like pattern in {0001} sector. There is no change in the pattern behaviour after rotation of the crystal. The longest diameter of the section is 1 mm. Crossed polars.

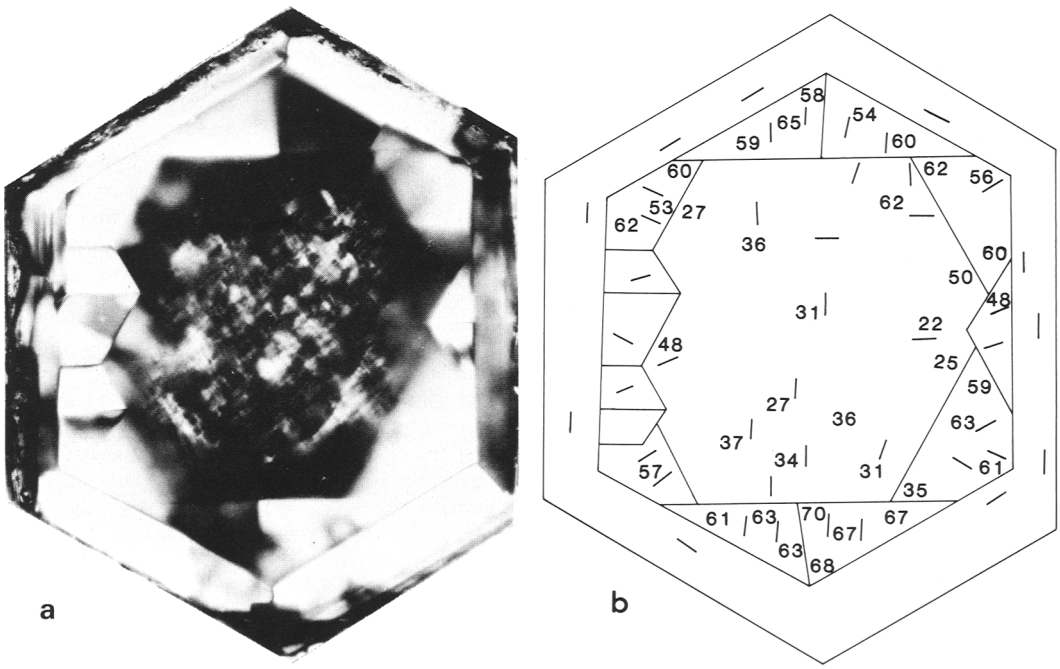

FIG. 2. (*a*) Optical sectors in the M1 crystal. The extinction angle of $\{10\bar{1}1\}$ sectors is 6°. Additional growth sectors are visible. The diameter of the crystal is 1 mm. Crossed polars. (*b*) 2V measurements and OAP orientations in optical sectors of the M1 crystal.

Refractive indices of the crystal labelled as M3 are: ω 1.535(2), ε 1.534(2). It should be noted, however, that the refractive indices seem to be slightly higher in pyramidal sectors than in prismatic and basal sectors as indicated by the Becke test.

The optic axial angle (2V) and orientations of the optic axial plane have been measured using a Zeiss universal stage for the M1 crystal and the data are summarized in fig. 2*b*. Because of patchy and undulose extinction it was in some cases difficult and often impossible to obtain interference figures of satisfactory quality, hence some of the 2V measurements are less accurate than others. In spite of this, a regularity in 2V distribution is clearly visible. The mean value of 2V for pyramidal sectors varies from 60 to 64° decreasing to 34° in the pinacoidal sector. In tourmaline and beryl smaller values of 2V in regions of crystals where cross-hatched twinning is present have also been observed (Foord and Mills, 1978).

Optic axial plane (OAP) azimuths generally reflect the external hexagonal symmetry of the crystal (fig. 2*b*) excluding the {0001} sector where the OAP orientations are apparently related to the cross-hatched pattern. The relationship between the OAP orientations and the crystallographic symmetry is different from the data given for other optically anomalous minerals (e.g. Foord and Mills, 1978; Scandale *et al.*, 1984) but in agreement with observations on milarites (e.g. Oftedal and Saebö, 1965; Chukhrov, 1981).

Growth structures. The growth structure in the Strzegom milarite is easily visible not only in thick sections parallel to the *c*-axis but also in uncut crystals when immersed in a refractive index liquid. The internal morphology of the Strzegom milarite suggests a steady growth rate (fig. 3). Sharply

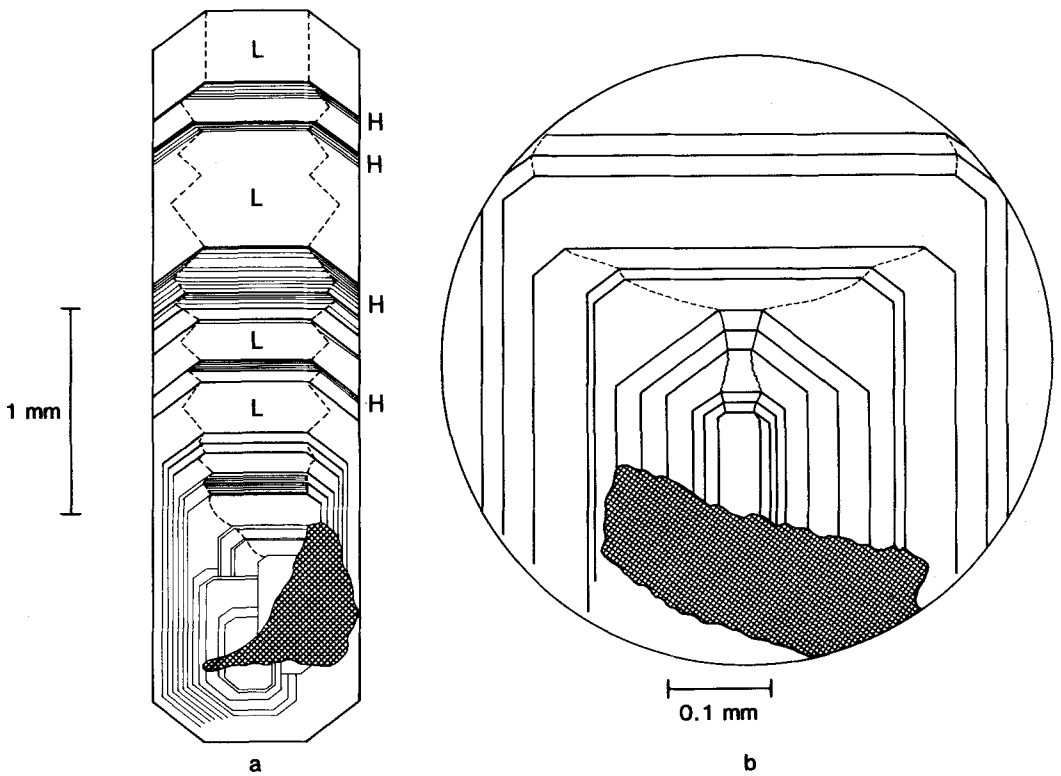

FIG. 3. Growth structure in milarite from Strzegom. (*a*) Crystal showing sharp growth layers grouped in high-birefringent bands (H) alternating with unstriated, low-birefringent regions (L). Dotted lines correspond to the lines of simultaneous growth of $(10\bar{1}1)$ and (0001) faces. The internal structure of the crystal reflect also the transport anisotropy during crystallization. Parallel growth of the milarite crystals at the early stage of crystallization is visible. (*b*) Details of the core of another crystal revealing the unequal development of $(10\bar{1}1)$ and (0001) faces during the crystal growth. Note the presence of stilpnomelane aggregates in cores of both crystals (shaded spots).

defined, high-birefringent growth layers are grouped in bands that alternate with low-birefringent regions of the crystal which do not show growth striation under the optical microscope. Obviously, homogeneous regions grew rapidly whereas anomalously high-birefringent bands reflect discontinuous growth events. All crystals have two or three extremely sharp boundaries between high-birefringent bands and homogenous regions, indicating at least three main stages of crystal growth.

In addition to the fluctuating growth rate of the whole crystal, rhythmic fluctuations of the growth rate of (0001) and (10$\bar{1}$1) faces took place resulting in characteristic saw-tooth like lines of simultaneous growth of these faces (fig. 3; see also fig. 1 in Janeczek, 1984). Identical structures have been described for milarite crystals from other localities (e.g. Chukhrov, 1981). Variations of growth rate of pinacoidal and pyramidal faces were particularly intensive in the early stage of the milarite crystallization (fig. 3*b*). Such a growth pattern indicates variations in the concentration gradient around the growing crystal in quiet hydrodynamic conditions. In other words, when, for instance, the (0001) faces grew rapidly the concentration of the constituent elements at the crystal-solution interface decreased, and the pyramidal faces started to grow faster, and so on. This process took place even if the crystals grew without interruption.

Electron microprobe analysis. Partial chemical analyses of crystals M1 and M2 cut perpendicular to the *c*-axis, as well as crystal M3 cut parallel to the *c*-axis, were performed with a Camebax microprobe. Link System ZAF-4 software for EDS analysis and software called 'Specta' for WDS analysis were used for data reduction.

The average results of chemical analyses are presented in Table I. Since it is not possible to determine Be and H_2O contents in minerals by means of the microprobe, the amount of Be in the milarite unit cell has been estimated on the basis of the charge balance (this procedure as well as calculation assuming Be–Al substitution leads to approximate results only).

It is not surprising that there is a discrepancy in chemical composition between the crystals, as variation on a very local scale is a typical feature of milarite. Nevertheless, the low Na_2O content and almost constant content of K_2O in all the samples examined is noteworthy. There are some isolated spots in the crystals were the Na_2O content is up to 0.5 wt. %, but there are also large regions, mainly within the {0001} sector, where the Na_2O content is below the detection limit of the energy dispersive system (EDS), i.e. less than 0.2 wt. %. Analyses of the M3 crystal obtained using the wavelength dispersive system (WDS) gave similar results,

Table I. Microprobe analyses of the Strzegom milarite

	M1		M2		M3	
SiO_2	72.55		72.41		73.04	
Al_2O_3	4.73		4.88		4.76	
FeO	0.00		n.d.		0.01	
MnO	0.12		n.d.		0.09	
CaO	10.78		11.11		10.92	
Na_2O	0.02[x]		0.00		0.04	
K_2O	4.71		4.66		4.60	
Total	92.91		93.06		93.46	
	a	b	a	b	a	b
Si	12.08	12.00	12.04	12.00	12.08	12.00
Al	0.93	0.92	0.96	0.95	0.93	0.92
Be_{calc}	2.00	2.19	2.00	2.10	2.00	2.19
Ca	1.92	1.91	1.98	1.97	1.93	1.92
Mn	0.02	0.02	-	-	0.01	0.01
K	1.00	0.995	0.99	0.985	0.97	0.96
Na	0.004	0.004	-	-	0.01	0.01

x - Na_2O contents vary from 0.0 to 0.5 wt.%

a - cations calculated on the basis of 28 oxygens

b - cations normalized to Si = 12.00

Table II. Variation of the chemical composition in optical sectors of the M1 crystal

	Sectors {1120}		{1011}		{0001}	
	wt.%	S.D.	wt.%	S.D.	wt.%	S.D.
Al_2O_3	4.87	0.18	4.74	0.25	4.72	0.20
CaO	10.84	0.22	10.83	0.27	10.63	0.17
K_2O	4.75	0.08	4.72	0.11	4.67	0.10

S.D. - standard deviation

confirming low sodium content in the Strzegom milarite. It should be also mentioned that a positive linear correlation between Al_2O_3 and SiO_2 (wt. %) has been established in the crystals studied.

Since the average data tell us nothing about compositional variability within a single crystal, microprobe analyses of the M1 sample were collected automatically for a grid spacing of 50 μm. The results are summarized in fig. 4. A correlation between chemical composition and optical sectors is not clear. The distribution of Al_2O_3, CaO and K_2O appears to be more uniform, and their contents are slightly lower in the {0001} sector than in others. This general tendency becomes more distinct when the average analytical data for single sectors are compared (Table II). Enrichment in Ca can be correlated with higher 2V and presumably with higher refractive indices in the pyramidal sectors. The increase of refractive indices of indivi-

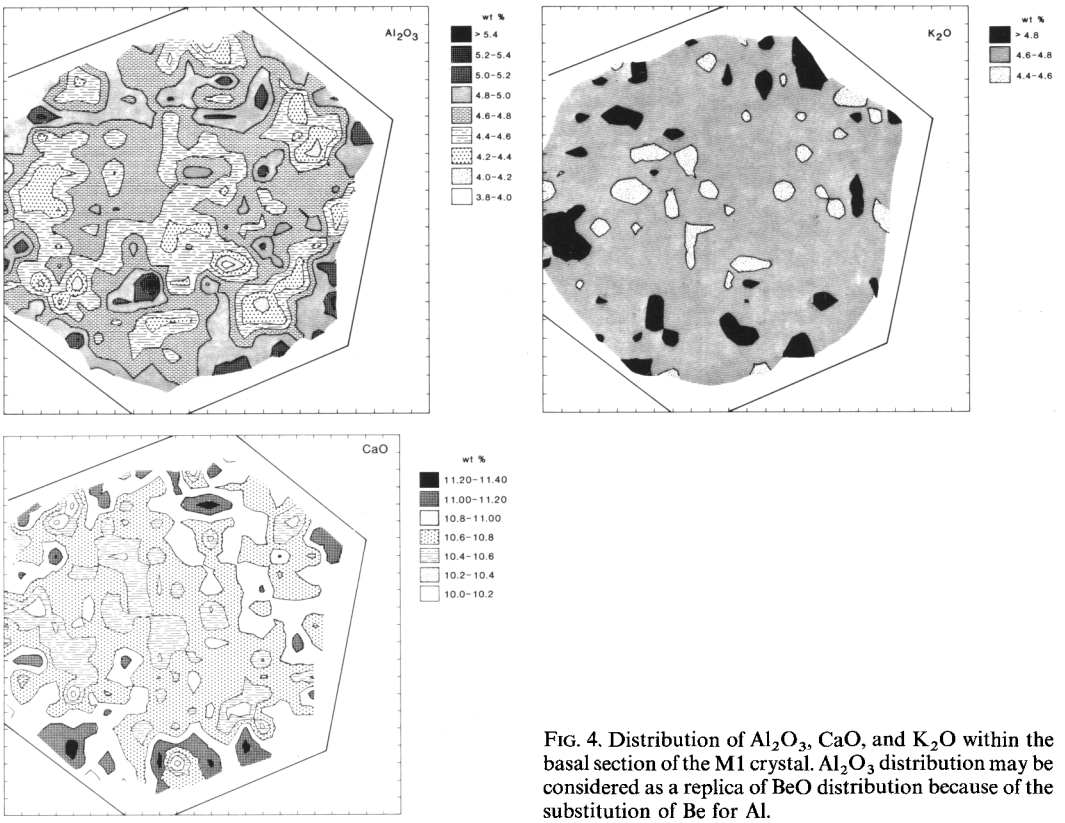

FIG. 4. Distribution of Al_2O_3, CaO, and K_2O within the basal section of the M1 crystal. Al_2O_3 distribution may be considered as a replica of BeO distribution because of the substitution of Be for Al.

dual zones in milarite with increasing Ca content has already been reported by Hügi and Röwe (1970). This trend can also be derived from data collected by Černy *et al.* (1980) although these authors paid attention mainly to the relationship between refractive indices and alkali plus water content. In contrast to other elements, K is distributed almost uniformly within the whole crystal and the deviation from its average content is negligible.

A microprobe scanning traverse of the M3 crystal was made along the *c*-axis at points 16 μm apart. There is no distinct correlation between growth structure and chemical composition of the crystal. It has been established, however, that in the outer part of the crystal, Al_2O_3 decreases slightly whereas Na_2O increases, apparently due to the substitution of Be for Al. Moreover, three bands enriched in MnO have been recognized but these cannot be correlated with distinct growth layers. The almost constant content of both Na_2O and K_2O along the crystal should be stressed. Therefore, these data do not confirm previous observations which have drawn attention to a considerable variability of the alkali content within a single crystal of milarite. For example, the differences in Na_2O and K_2O contents between growth pyramids of {0001} and $\{11\bar{2}0\}$ equal 0.19 and 0.87 wt. % respectively have been reported for milarite showing an hour-glass structure (Chistyakova *et al.* 1964).

The presence of water molecules in the Strzegom milarite has been proved by the infra-red absorption analysis (fig. 5). Very weak and broad absorption centred at 3160 cm^{-1} (not shown in fig. 5) and broadening of the absorption band at 3550 cm^{-1} suggests H-bonding of H_2O molecules.

Y and Ar have been qualitatively determined in the crystal M4 by means of the analytical electron microscope. Ar is presumably located in channels of the milarite structure.

Optical anomalies. The origin of biaxial optical sectors in milarite has been discussed by Černy *et al.* (1980), who emphasized the role of sectorial chemical substitutions in generating the biaxiality and other types of anomalies. As they suggested 'the

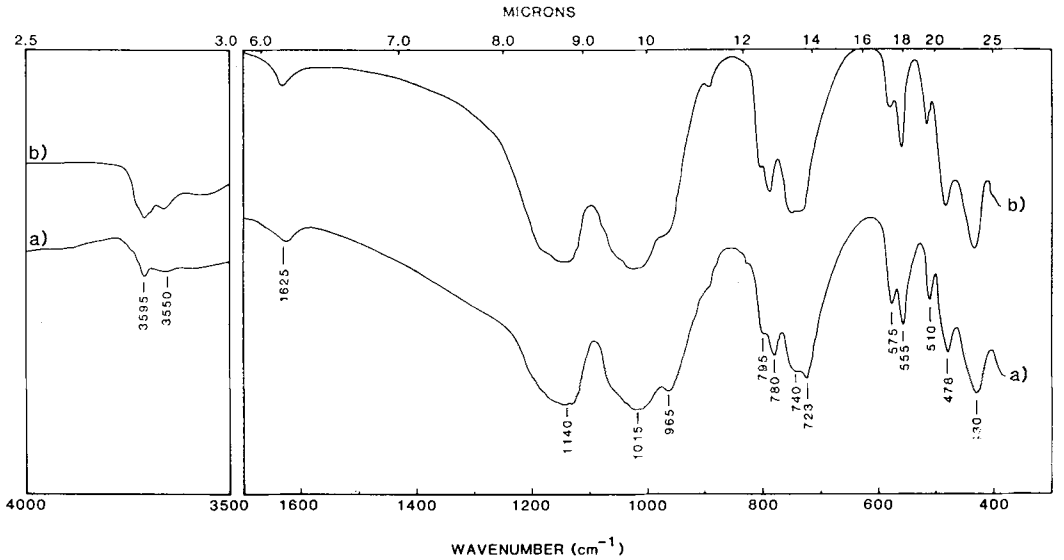

FIG. 5. Infra-red spectra of milarite from (*a*) Strzegom, (*b*) Guanajuato, Mexico. Perkin Elmer 397 spectrometer (KBr plates and Nujol mull).

dimensional misfit may be expected along boundaries of sectors with different water contents, resulting in strain and optical anomalies . . .'

In the case of the Strzegom milarite, high birefringence of distinctly striated growth bands indicates that a certain strain is associated with inhomogeneous regions of the crystals, whereas regions with low (normal) birefringence are strain-free. These alternating parts of the crystal will probably have slightly different elasto-optical properties, hence they may act as two or more superimposed crystals producing a Moiré-like pattern when viewed under polarized light. High resolution transmission electron microscopy (HRTEM) of the M4 crystal showing a Moiré-like pattern has revealed an undistorted lattice with a few dislocations only. Electron diffraction patterns of the crystal do not show any deviation from the *P6/mcc* space group. Therefore, one can conclude that in the case of the Strzegom milarite the optical patterns are caused by internal strain induced by the inhomogeneous growth rate of crystals.

It should be noted that stilpnomelane aggregates included in the cores of the milarite crystals have produced strain which is very often relieved in cracks surrounded by a tartan-like optical pattern visible even in uncut crystals.

Hydrothermal experiments with armenite, which is closely related to milarite, seem to indicate that the bulk water content does not play a major role in producing optical anomalies. Hydrothermally treated armenite became uniaxial and optical patterns disappeared, whereas the water content remained unchanged (Pouliot *et al.*, 1984). By analogy with armenite a similar behaviour of milarite may be expected. Unfortunately the water content in single sectors of crystals cannot be yet determined, so we are not able to accept entirely or reject the hypothesis of Černy *et al.* (1980). In optically anomalous crystals of different minerals, a distinct correlation between optic axial angles and chemical composition could not be found (Foord and Mills, 1978; Goldman and Rossman, 1978; Pouliot *et al.*, 1984). However, the channel population greatly affects the anomalous biaxiality in osumilite—another mineral belonging to the milarite group (Goldman and Rossman, 1978) and cordierite (Armbruster and Bloss, 1981). Presumably positional disorder of the channel constituents rather than their content may be essential for the optical behaviour of these minerals. Černy *et al.* (1980) have mentioned possible disorder of both Ca and H_2O but this assumption was not confirmed by their infra-red absorption data. The structural analysis of synthetic Mn-milarite revealed the presence of twelve weak reflections on its X-ray pattern, violating the *P6/mcc* space group (a new space group has not been given). This lowering of symmetry has been explained as a result of the water molecule displacement with the possible formation of a hydrogen bond (Sandomirskij *et al.*, 1977). The fact that additional reflections have

appeared on X-ray patterns of synthetic Mn-milarite whereas natural milarites do not show lower X-ray symmetry may indicate not only a different chemical composition, but also a difference in the crystal growth history.

Pouliot *et al.* (1984) have suggested the presence of a modulated structure in armenite as a result of ordering of the channel and interchannel constituents. Direct lattice images obtained in this study argue against that supposition. There is no evidence for the existence of ordered domains in milarite, and anomalous optical microstructures can be explained in terms of the inhomogeneous crystal growth.

Finally, we must state that the real reason for the sectorial biaxiality in milarite, as well as in other minerals belonging to the milarite group, is still uncertain. In the case of the Strzegom milarite, the distinct optical sectors are not related to the chemical sector zoning in spite of the fact that the distribution of SiO_2, Al_2O_3, and CaO is far from uniform. Since there is no significant compositional variation along the length of elongated crystals, it can be concluded that their complicated growth structure reflects fluctuations of the concentration flux or temperature oscillations.

Primary internal strain responsible for the anomalous biaxiality in many minerals may be induced by several processes such as cation ordering, sectorial chemical substitution, distribution of impurities and so on. However, all these processes depend on crystal growth mechanisms (e.g. Akizuki, 1981; Scandale *et al.*, 1984). Therefore, further study on milarite should perhaps devote more attention to the growth history of this mineral.

Acknowledgements. I acknowledge use of the research facilities of the Department of Geology, University of Manchester, made available to me while I was on the British Council scholarship. I am particularly grateful to Prof. W. S. MacKenzie for his help in the optical study, encouragement and stimulating discussions. My sincere thanks are due to Dr M. Dorling for her help throughout the work and HRTEM investigations. I wish to thank T. Hopkins and D. Plant for their assistance in the microprobe analyses. I am indebted to Dr W. T. C. Sowerbutts for computer maps of the element distributions and to Dr. R. S. W. Braithwaite of UMIST who performed IR analysis of the Strzegom milarite and kindly provided me with a spectrum of the Guanajuato milarite.

REFERENCES

Akizuki, M. (1981) *Am. Mineral.* **66,** 403–9.
Armbruster, T., and Bloss, F. D. (1981) *Contrib. Mineral. Petrol.* **77,** 332–6.
Bakanin, V. V., Balko, V. P., and Solovyeva, L. P. (1974) *Sov. Phys. Crystallogr.* **19,** 460–2.
Černy, P., Hawthorne, F. C., and Jarosewich, E. (1980) *Can. Mineral.* **18,** 41–57.
Chistyakova, M. B., Osolodkina, G. A., and Razmanova, Z. P. (1964) *Dokl. Akad. Nauk SSSR* **159,** 1305–8.
Chukhrov, F. V., ed. (1981) *Mineraly, Nauka, Moscow,* **3,** part 2, 143–50.
Foord, E. E., and Mills, B. A. (1978) *Am. Mineral.* **63,** 316–25.
Goldman, D. S., and Rossman, G. R. (1978) Ibid. **63,** 490–8.
Hügi, T., and Röwe, D. (1970) *Schweiz. Mineral. Petrog. Mitt.* **50,** 445–80.
Janeczek, J. (1984) *Przegląd Geol.* **3,** 165–7.
Oftedal, I., and Saebö, P. C. (1965) *Norsk Geol. Tidsskr.* **45,** 171–5.
Pouliot, G., Trudel, P. Valiquett, G., and Samso, P. (1984) *Can. Mineral.* **22,** 453–64.
Sandomirskij, P. A., Simonov, M. A., and Belov, N. V. (1977) *Soviet Phys. Dokl.* **22,** 453–64.
Scandale, E., Lucchesi, S., and Graziani, G. (1984) *Phys. Chem. Minerals,* **11,** 60–6.

[*Manuscript received 8 July 1985; revised 12 November 1985*]